Supporting Information

Supporting Methods

Protein expression and purification. Strep-tagII-tagged GlnK (stGlnK) was expressed and purified as previously described (1). Unless otherwise stated, all purification steps were carried out at 4 °C. To purify functional, highly-purified AmtB, purified tagless AmtB and stGlnK were mixed at a molar ratio of 1:3 in GF buffer (50 mM TRIS pH 7.4 at room temperature, 100 mM sodium chloride, 10% glycerol, 0.025% DDM and 1 mM ADP) and incubated overnight. The mixture of AmtB and stGlnK was loaded onto a StrepTrap HP 5 mL column (GE Healthcare) to capture AmtB in complex with stGlnK, and flow through contained non-functional AmtB. Bound protein was eluted with the same buffer containing 2.5 mM D-desthiobiotin, concentrated, incubated overnight with apyrase (New England Biolabs) to dissociate the complex, and loaded onto a Superdex 200 Increase 10/300 GL column (GE Healthcare) equilibrated in GF buffer supplemented with 0.5% C_8E_4 instead of DDM. Peak fractions containing the functional AmtB were pooled, concentrated, flash frozen in liquid nitrogen, and stored at -80 °C. Protein concentration was determined using the DC Protein Assay kit (Bio-Rad) using bovine serum albumin as the standard for protein concentration. The H156A mutant of AmtB was achieved by site-directed mutagenesis using a QuikChange Lightning Site-Directed Mutagenesis Kit (Stratagene) according to manufacturer's protocol. AmtB mutants were expressed and purified as described for the wild-type protein. For co-crystallization trials, AmtB was expressed and purified as previously described (1, 2). AqpZ was expressed and prepared as previously described (2).

Preparation and titration of phospholipids. Phospholipid samples of 1-palmitoyl-2-oleoyl-sn-glycero-3-phosphocholine (POPC), 1-palmitoyl-2-oleoyl-sn-glycero-3-phospho-(1'-rac-glycerol) (POPG), 1-palmitoyl- 2-oleoyl-sn-glycero-3-phosphoethanolamine (POPE), 1-palmitoyl-2-oleoyl-sn-glycero-3-phosphate (POPA), 1-palmitoyl-2-oleoyl-sn-glycero-3-phospho-L-serine (POPS), 1,1',2,2'-tetraoleoyl-cardiolipin (TOCDL), and 1,1',2,2'-tetraoleoyl cardiolipin[4-(dipyrromethene boron difluoride)butanoyl] (TFCDL) were obtained from Avanti Polar Lipids Inc., Alabama, USA. Stock solutions of each lipid were prepared in AA buffer (200 mM ammonium acetate) containing 2x critical micelle concentration (CMC) of tetraethylene glycol monooctyl ether (C_8E_4) as previously described (1). Phospholipid concentration was determined by phosphorus analysis (3, 4). The protein-lipid mixture was then loaded into a gold-coated capillary (5), followed by equilibration for five minutes in the source chamber of the mass spectrometer set at a given temperature using a temperature-controlled source(1) before recording mass spectra. As reported previously (1), no significant differences in mole fractions of lipid(s) bound to AmtB was observed with longer incubation times of up to 24 hours. For each dilution series, a lipid (light or heavy) was set to a constant concentration while the concentration of the other lipid was varied, typically 6 to 8 concentrations.

Second-generation temperature-controlled source. Samples of AmtB at a final concentration of 2.1 μM combined with lipid(s) were analyzed at a given temperature using a second-generation temperature-controlled source with improved cooling and heating capabilities. Building off our previous design (1), two 120 mm central processing unit (CPU) fans (Antec-TriCool) were fixed to the source chamber of a Synapt G1 HDMS mass spectrometer (Waters) to direct temperature-controlled air over the sample capillary to modulate source temperature. Control of the air

temperature was achieved by flowing ambient air into a large insulated chamber that was affixed with an air cooler device (Model no. AC-162, TE Technology) controlled by a bipolar thermoelectric temperature controller (Model no. TC-720, TE Technology). Source air temperature was recorded and calibration of sample temperature were performed as described previously (1).

Identification of suitable lipid pairs. For a given lipid pair consisting of a light and heavy adduct, the mass spectrum was simulated using custom Python scripts and took advantage of a Python function for predicting mass spectra from the program Pulsar (6). The mass for combinations of the lipid binding events was calculated and added to the apo protein mass. In addition, the number of permutations per combination was used to convert intensities to fractional percentage for all combinations for a particular number of lipids bound. For a given lipid pair, the minimum intensity values across the m/z range for the comparison of all theoretical mass spectra corresponding to apo and different lipid bound states of up to five bound in total was calculated. Summation of the step-wise comparisons of mass spectra resulted in the peak overlap as shown in Fig. S1A and S1C.

Native mass spectrometry analysis. Nano electrospray ionization was performed using gold coated capillaries prepared in house as previously described (5). Purified protein was buffer exchanged into AA buffer containing 0.5% C_8E_4 for native mass MS experiments as previously described (2). For AmtB-lipid binding studies, instrument parameters were tuned to maximize ion intensity but simultaneously preserve the native-like state of AmtB as determined by ion mobility. The instrument was set to a capillary voltage of 1.7 kV, source temperature of 90 °C, sampling cone voltage of 150-200 V, extraction cone voltage of 10 V, trap collision energy 50-150 V, transfer collision energy 10 – 50 V, and argon flow rate at 7 ml/min (5.2 x 10-2 mbar). The T-wave settings for trap (300 ms-1/2.0 V), IMS (300 ms-1/20 V) and transfer (100 ms-1/10 V), source temperature (90 °C) and trap bias (25-35 V) were optimized.

AmtB crystallization and structure determination. Molecular replacement models displayed a single AmtB subunit within the asymmetric unit. Strong positive density ($\sigma > 10$) was observed in the difference maps (F_o-F_c) in the vicinity of residue N73 of AmtB, which correlated well to a phosphate group of TFCDL. Additional positive density ($\sigma>7$) was observed ~3.4 and 7.1Å away from this position, which correlated well to the glycerol backbone and the second phosphate group of TFCDL.

Supporting Figures

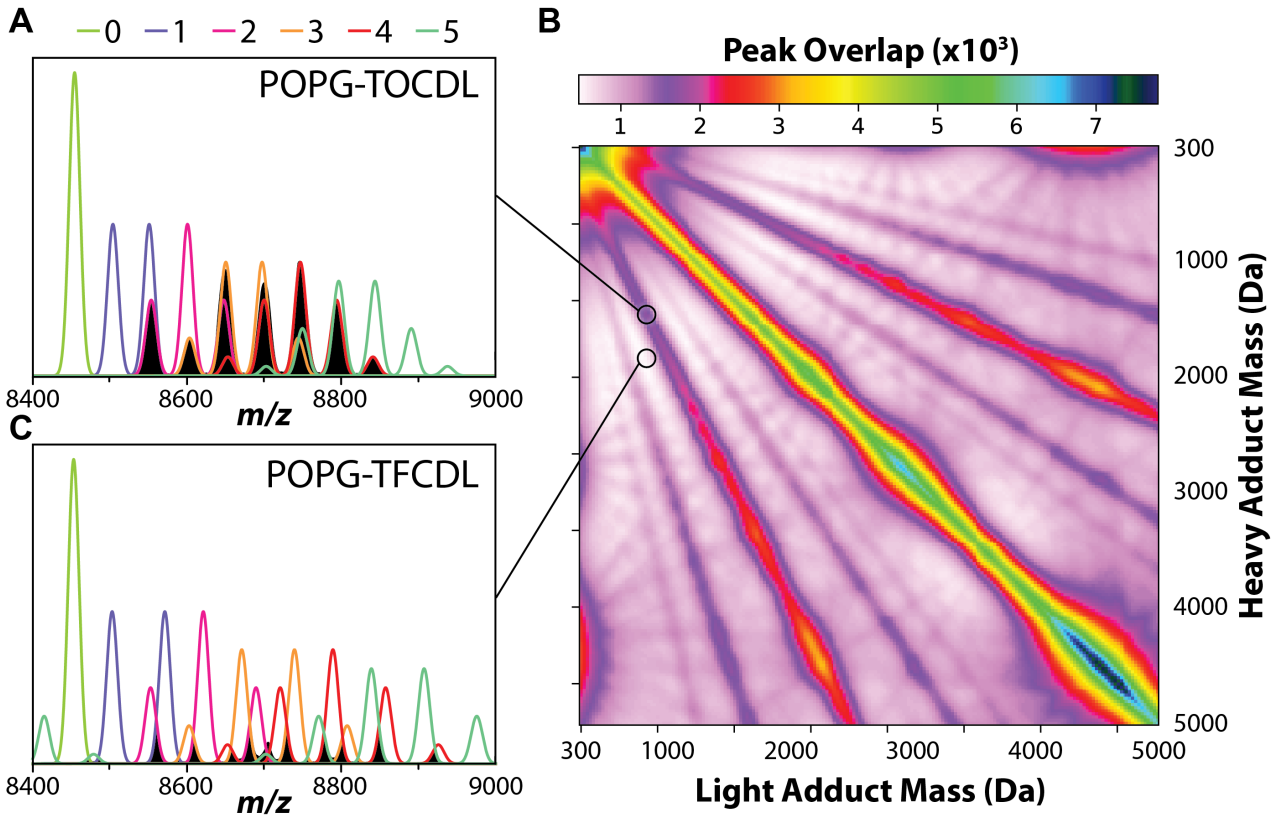

Figure S1 | Theoretical mass spectra for heterolipids binding AmtB identifies resolvable lipid pairs. Mass spectra were generated using the experimental mass resolution for AmtB obtained on an Synapt G1 instrument (Waters) and up to five lipids bound in total were considered. A) The 14^{+}charge state of apo AmtB and bound to POPG and TOCDL and combinations thereof. The black filled peaks correspond to the peak overlap (see Supporting Methods) for predicted mass spectra. B) Plot of peak overlap for lipid pairs containing a light and heavy adduct ranging in mass from 300 to 5000 Da. C) Mass spectrum for the lipid pair, POPG and TFCL reveals marginal peak overlap, and shown as in A. The additional mass afforded by the BODIPY group covalently attached to TFCDL provides the necessary mass shift such that it can be resolved from other natural phospholipids found in *Escherichia coli*.

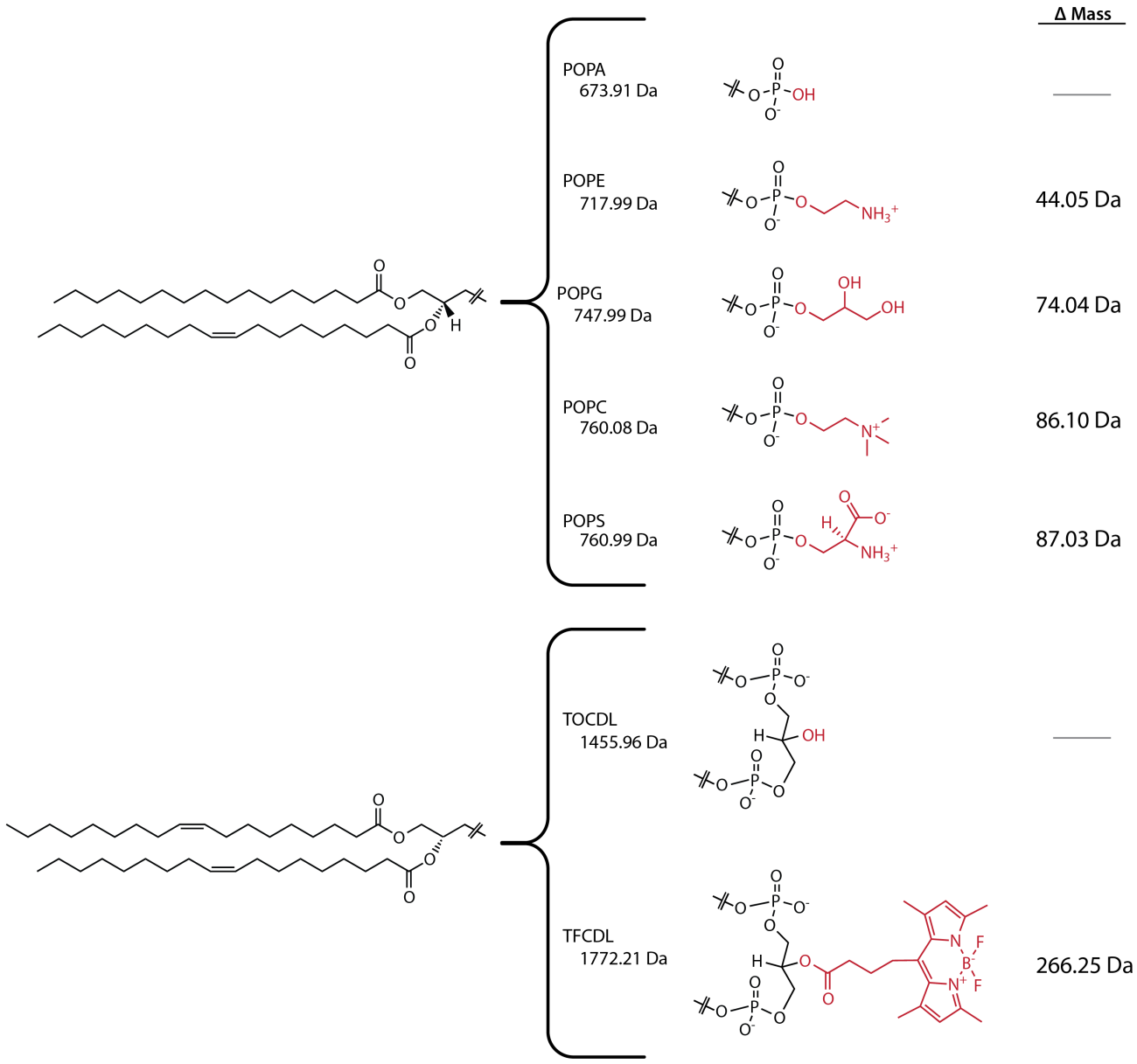

Figure S2 | Phospholipid structures and abbreviations used in this study. The difference between headgroups are colored red and their mass differences tabulated.

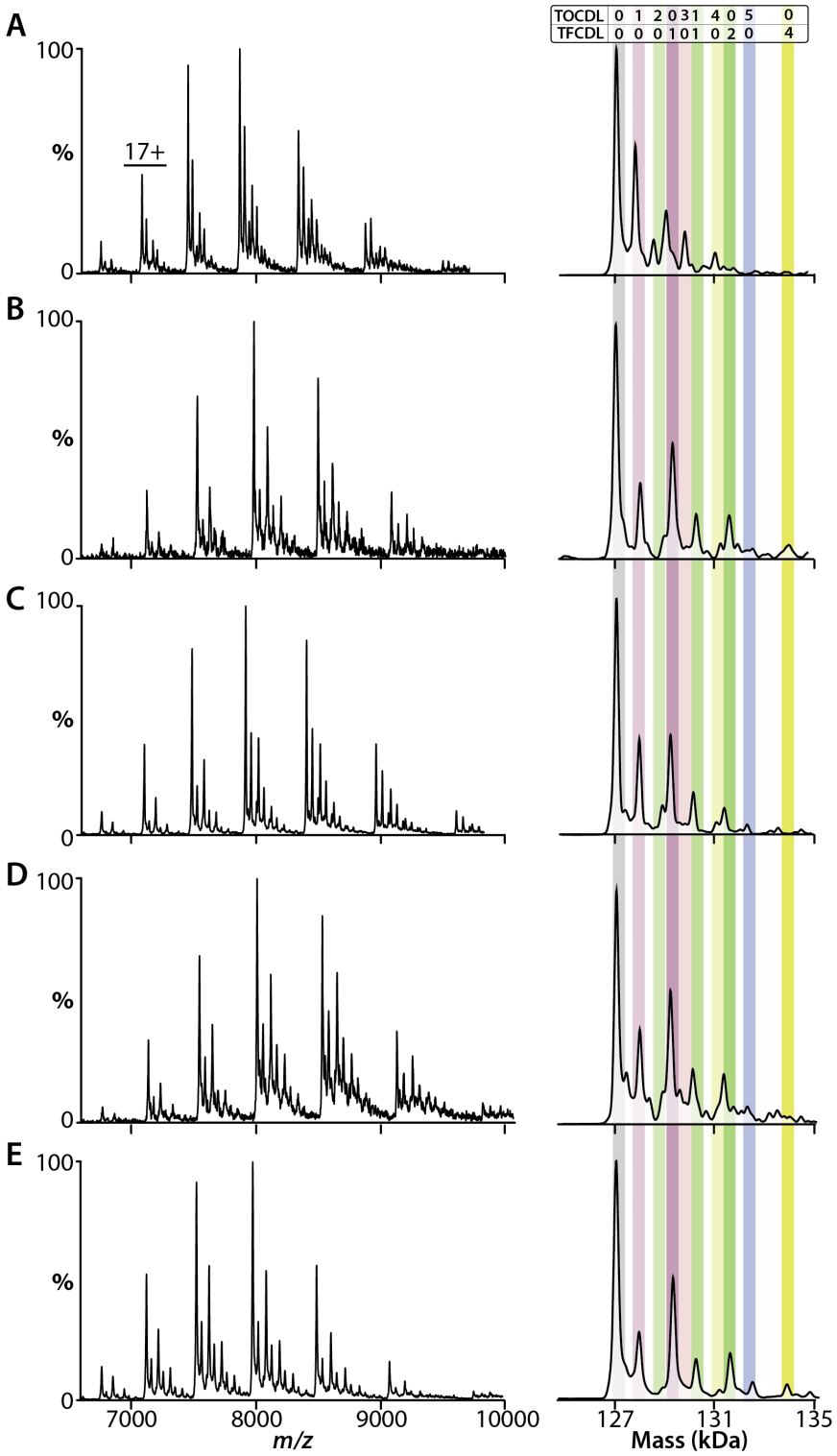

Figure S3 | Representative mass spectra and deconvolution for different lipid pairs bound to AmtB. The panel to the right shows the deconvolution of the mass spectrum to the left and number of TFCDL and other lipids bound to AmtB. From top to bottom, AmtB mixed with TFCDL and either (A) POPA, (B) POPC, (C) POPG, (D) POPE, and (E) POPS. Shown to the right is the deconvoluted mass spectrum.

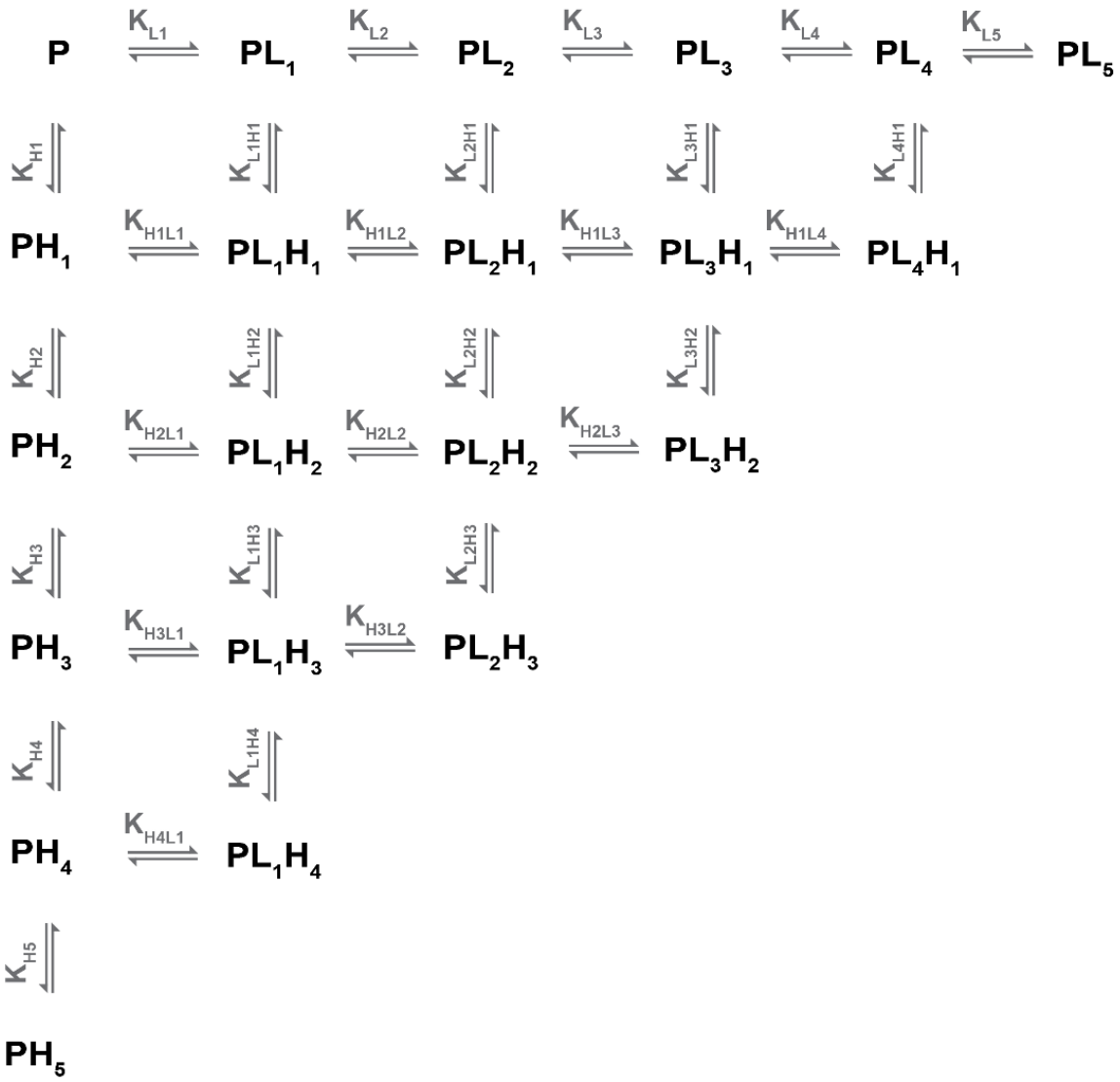

Figure S4 | Equilibrium binding model for two different lipids binding AmtB (P). L and H designate binding of either a light or heavy lipid, which is defined by their molecular weight respectively.

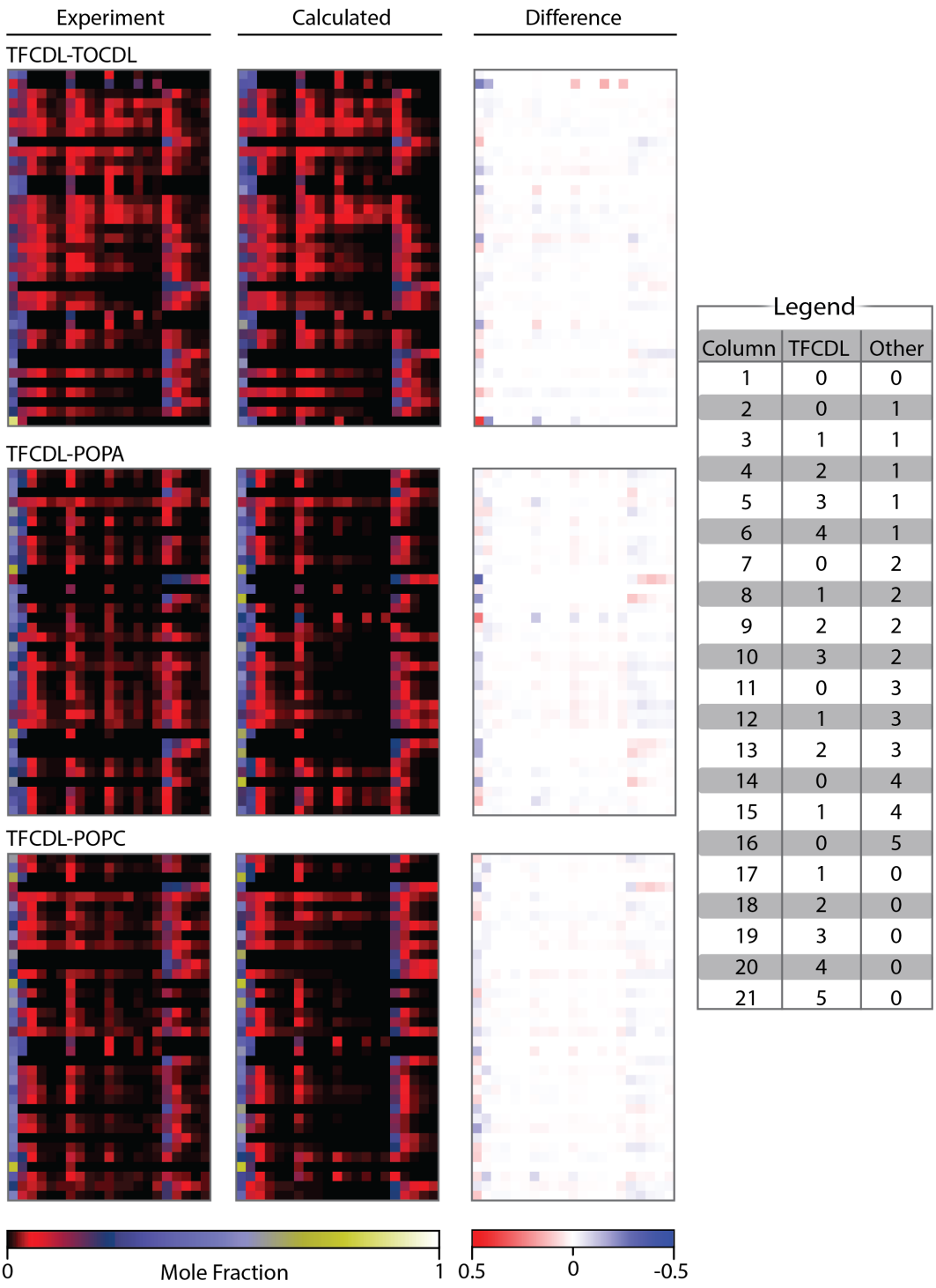

Legend

Column	TFCDL	Other
1	0	0
2	0	1
3	1	1
4	2	1
5	3	1
6	4	1
7	0	2
8	1	2
9	2	2
10	3	2
11	0	3
12	1	3
13	2	3
14	0	4
15	1	4
16	0	5
17	1	0
18	2	0
19	3	0
20	4	0
21	5	0

Figure S5 | Representative matrix plots for experimental data and fit of coupled equilibrium model for AmtB bound to lipid pairs: TFCDL·TOCDL, TFCDL·POPA, and TFCDL·POPC. The X axis represents apo and different lipid bound species of AmtB (see legend) whereas the Y axis represents a titrant from the titration series. Shown to the right is the difference between experimental minus calculated mole fractions.

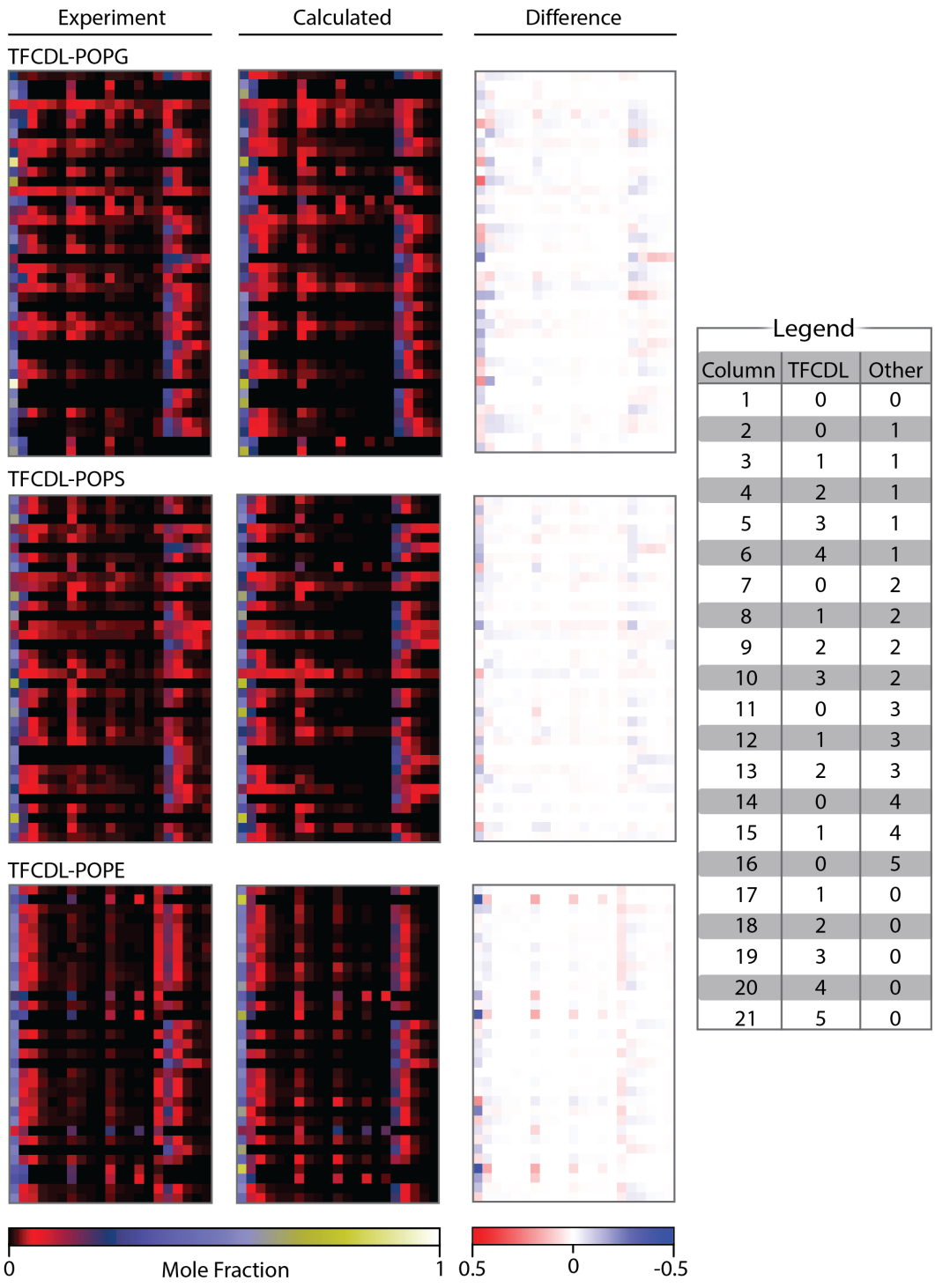

Figure S6 | Representative matrix plots for experimental data and fit of coupled equilibrium model AmtB bound to lipid pairs: TFCDL·POPG, TFCDL·POPS, TFCDL·POPE. Figure is shown as in Supplementary Information Figure 5.

A

Lipid Species	k_D (μM)
$KPOPA_1$	7.8 ± 0.02
$KPOPA_2$	16.9 ± 0.18
$KPOPA_3$	27.1 ± 2.00
$KPOPA_4$	25.2 ± 0.60
$KPOPA_5$	17.4 ± 3.23
$KTFCDL_1$	15.4 ± 0.52
$KTFCDL_2$	13.3 ± 0.71
$KTFCDL_3$	20.1 ± 2.38
$KTFCDL_4$	14.9 ± 2.30
$KTFCDL_5$	10.2 ± 1.61
$KPOPA_1TFCDL_1$	13.9 ± 0.27
$KPOPA_1TFCDL_2$	19.5 ± 0.53
$KPOPA_1TFCDL_3$	21.9 ± 2.75
$KPOPA_1TFCDL_4$	8.5 ± 1.76
$KPOPA_2TFCDL_1$	13.2 ± 0.48
$KPOPA_2TFCDL_2$	22.3 ± 1.87
$KPOPA_2TFCDL_3$	10.7 ± 1.42
$KPOPA_3TFCDL_1$	8.7 ± 1.03
$KPOPA_3TFCDL_2$	21.9 ± 5.02
$KPOPA_4TFCDL_1$	14.8 ± 4.54

Lipid Species	k_D (μM)
$KPOPC_1$	12.4 ± 0.29
$KPOPC_2$	19.4 ± 0.46
$KPOPC_3$	27.0 ± 1.62
$KPOPC_4$	28.8 ± 2.92
$KPOPC_5$	14.1 ± 0.91
$KTFCDL_1$	10.2 ± 0.18
$KTFCDL_2$	14.4 ± 0.54
$KTFCDL_3$	15.4 ± 0.48
$KTFCDL_4$	16.9 ± 1.85
$KTFCDL_5$	10.0 ± 1.20
$KPOPC_1TFCDL_1$	11.9 ± 0.08
$KPOPC_1TFCDL_2$	15.2 ± 1.01
$KPOPC_1TFCDL_3$	15.6 ± 0.53
$KPOPC_1TFCDL_4$	9.4 ± 1.53
$KPOPC_2TFCDL_1$	10.2 ± 0.88
$KPOPC_2TFCDL_2$	10.7 ± 0.48
$KPOPC_2TFCDL_3$	11.7 ± 0.40
$KPOPC_3TFCDL_1$	7.2 ± 0.86
$KPOPC_3TFCDL_2$	12.2 ± 3.20
$KPOPC_4TFCDL_1$	11.2 ± 2.36

Lipid Species	k_D (μM)
$KPOPG_1$	13.3 ± 0.09
$KPOPG_2$	18.8 ± 0.20
$KPOPG_3$	22.4 ± 1.19
$KPOPG_4$	30.8 ± 0.78
$KPOPG_5$	15.1 ± 1.03
$KTFCDL_1$	10.0 ± 0.15
$KTFCDL_2$	14.9 ± 0.12
$KTFCDL_3$	22.6 ± 0.63
$KTFCDL_4$	25.2 ± 1.32
$KTFCDL_5$	17.0 ± 0.51
$KPOPG_1TFCDL_1$	11.2 ± 0.10
$KPOPG_1TFCDL_2$	15.8 ± 1.12
$KPOPG_1TFCDL_3$	19.4 ± 1.53
$KPOPG_1TFCDL_4$	23.4 ± 1.15
$KPOPG_2TFCDL_1$	9.5 ± 0.27
$KPOPG_2TFCDL_2$	16.2 ± 0.76
$KPOPG_2TFCDL_3$	17.4 ± 2.57
$KPOPG_3TFCDL_1$	7.9 ± 0.41
$KPOPG_3TFCDL_2$	16.3 ± 1.19
$KPOPG_4TFCDL_1$	8.0 ± 0.92

Lipid Species	k_D (μM)
$KPOPS_1$	9.4 ± 4.65
$KPOPS_2$	16.6 ± 7.70
$KPOPS_3$	29.5 ± 10.73
$KPOPS_4$	27.1 ± 8.65
$KPOPS_5$	12.0 ± 3.83
$KTFCDL_1$	5.7 ± 2.78
$KTFCDL_2$	8.6 ± 4.04
$KTFCDL_3$	8.7 ± 4.17
$KTFCDL_4$	9.0 ± 3.81
$KTFCDL_5$	6.9 ± 2.84
$KPOPS_1TFCDL_1$	5.1 ± 2.47
$KPOPS_1TFCDL_2$	8.5 ± 3.84
$KPOPS_1TFCDL_3$	7.0 ± 3.47
$KPOPS_1TFCDL_4$	6.3 ± 2.83
$KPOPS_2TFCDL_1$	4.0 ± 1.69
$KPOPS_2TFCDL_2$	8.0 ± 3.38
$KPOPS_2TFCDL_3$	5.4 ± 2.39
$KPOPS_3TFCDL_1$	2.4 ± 1.01
$KPOPS_3TFCDL_2$	6.7 ± 3.13
$KPOPS_4TFCDL_1$	3.1 ± 0.62

Lipid Species	k_D (μM)
$KTOCDL_1$	3.2 ± 1.53
$KTOCDL_2$	5.3 ± 2.36
$KTOCDL_3$	7.2 ± 3.38
$KTOCDL_4$	8.3 ± 3.91
$KTOCDL_5$	8.0 ± 3.73
$KTFCDL_1$	5.0 ± 2.31
$KTFCDL_2$	7.8 ± 3.64
$KTFCDL_3$	9.8 ± 4.30
$KTFCDL_4$	11.9 ± 4.99
$KTFCDL_5$	8.3 ± 3.30
$KTOCDL_1TFCDL_1$	4.2 ± 1.94
$KTOCDL_1TFCDL_2$	6.9 ± 3.27
$KTOCDL_1TFCDL_3$	8.3 ± 3.77
$KTOCDL_1TFCDL_4$	9.7 ± 4.33
$KTOCDL_2TFCDL_1$	3.8 ± 1.69
$KTOCDL_2TFCDL_2$	5.4 ± 2.55
$KTOCDL_2TFCDL_3$	7.7 ± 3.72
$KTOCDL_3TFCDL_1$	3.5 ± 1.49
$KTOCDL_3TFCDL_2$	5.5 ± 2.42
$KTOCDL_4TFCDL_1$	3.4 ± 1.54

Lipid Species	k_D (μM)
$KPOPE_1$	8.4 ± 0.06
$KPOPE_2$	9.1 ± 0.31
$KPOPE_3$	4.2 ± 0.23
$KPOPE_4$	8.5 ± 0.21
$KPOPE_5$	8.6 ± 0.61
$KTFCDL_1$	8.6 ± 0.22
$KTFCDL_2$	11.4 ± 0.23
$KTFCDL_3$	12.5 ± 0.60
$KTFCDL_4$	17.9 ± 0.68
$KTFCDL_5$	9.7 ± 1.05
$KPOPE_1TFCDL_1$	8.1 ± 0.22
$KPOPE_1TFCDL_2$	9.4 ± 0.28
$KPOPE_1TFCDL_3$	7.2 ± 0.18
$KPOPE_1TFCDL_4$	3.9 ± 0.11
$KPOPE_2TFCDL_1$	10.0 ± 0.77
$KPOPE_2TFCDL_2$	5.5 ± 2.91
$KPOPE_2TFCDL_3$	N/A
$KPOPE_3TFCDL_1$	8.8 ± 0.99
$KPOPE_3TFCDL_2$	9.3 ± 5.09
$KPOPE_4TFCDL_1$	N/A

B

	POPA	POPC	POPG	POPS	TOCDL	POPE
α(1,1)	1.1 ± 0.04	0.9 ± 0.02	0.9 ± 0.03	1.1 ± 0.02	1.2 ± 0.02	1.1 ± 0.03
α(2,1)	1.1 ± 0.03	1.2 ± 0.10	1.2 ± 0.08	1.3 ± 0.04	1.1 ± 0.05	0.8 ± 0.04
α(3,1)	1.6 ± 0.22	1.4 ± 0.16	1.2 ± 0.18	1.9 ± 0.04	1.1 ± 0.04	1.2 ± 0.07
α(4,1)	0.7 ± 0.25	0.7 ± 0.07	1.0 ± 0.19	0.8 ± 0.10	1.0 ± 0.06	0.0 ± 0.00
α(1,2)	0.7 ± 0.05	1.0 ± 0.09	1.0 ± 0.04	1.0 ± 0.06	1.1 ± 0.07	1.2 ± 0.05
α(2,2)	0.9 ± 0.05	1.4 ± 0.16	1.0 ± 0.03	1.1 ± 0.03	1.3 ± 0.07	0.8 ± 0.42
α(1,3)	0.9 ± 0.07	1.0 ± 0.01	1.2 ± 0.02	1.2 ± 0.11	1.1 ± 0.03	1.7 ± 0.10
α(2,3)	2.2 ± 0.48	1.3 ± 0.08	1.1 ± 0.06	1.4 ± 0.11	1.0 ± 0.03	0.0 ± 0.00
α(1,4)	1.8 ± 0.15	1.9 ± 0.47	1.1 ± 0.03	1.4 ± 0.11	1.2 ± 0.02	4.6 ± 0.28

Figure S7 | Equilibrium binding constants and coupling factors for different lipid pairs binding AmtB. Reported are the average and s.e.m. from repeated measurements (n = 3).

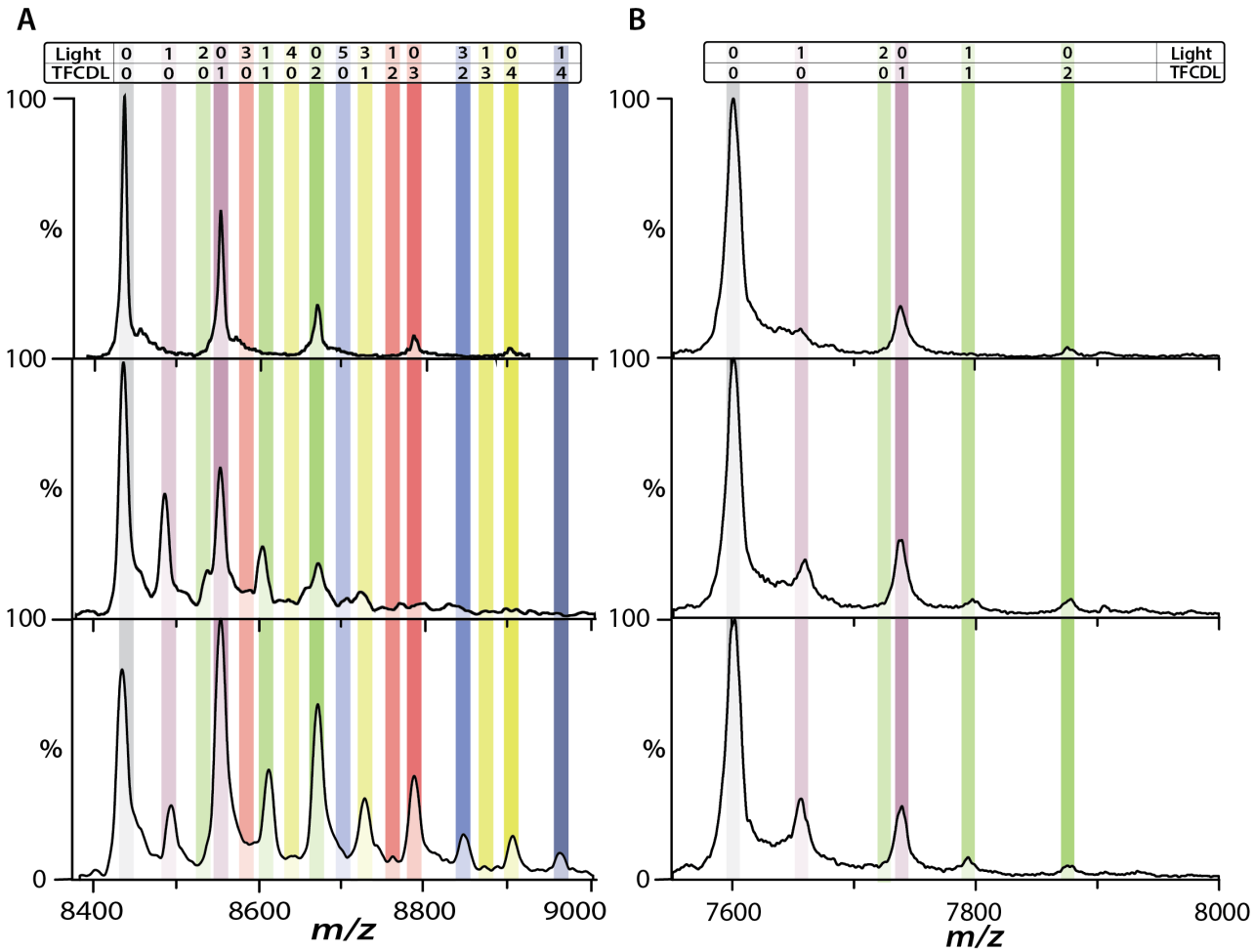

Figure S8 | Native mass spectra of AmtB and AqpZ in the presence of TFCDL, POPE, and POPC. Enlargement of (A) the 15^{+} charge state of AmtB and (B) the 13^{+} charge state of AqpZ. Lipid bound states are shown as in Fig. 2B.

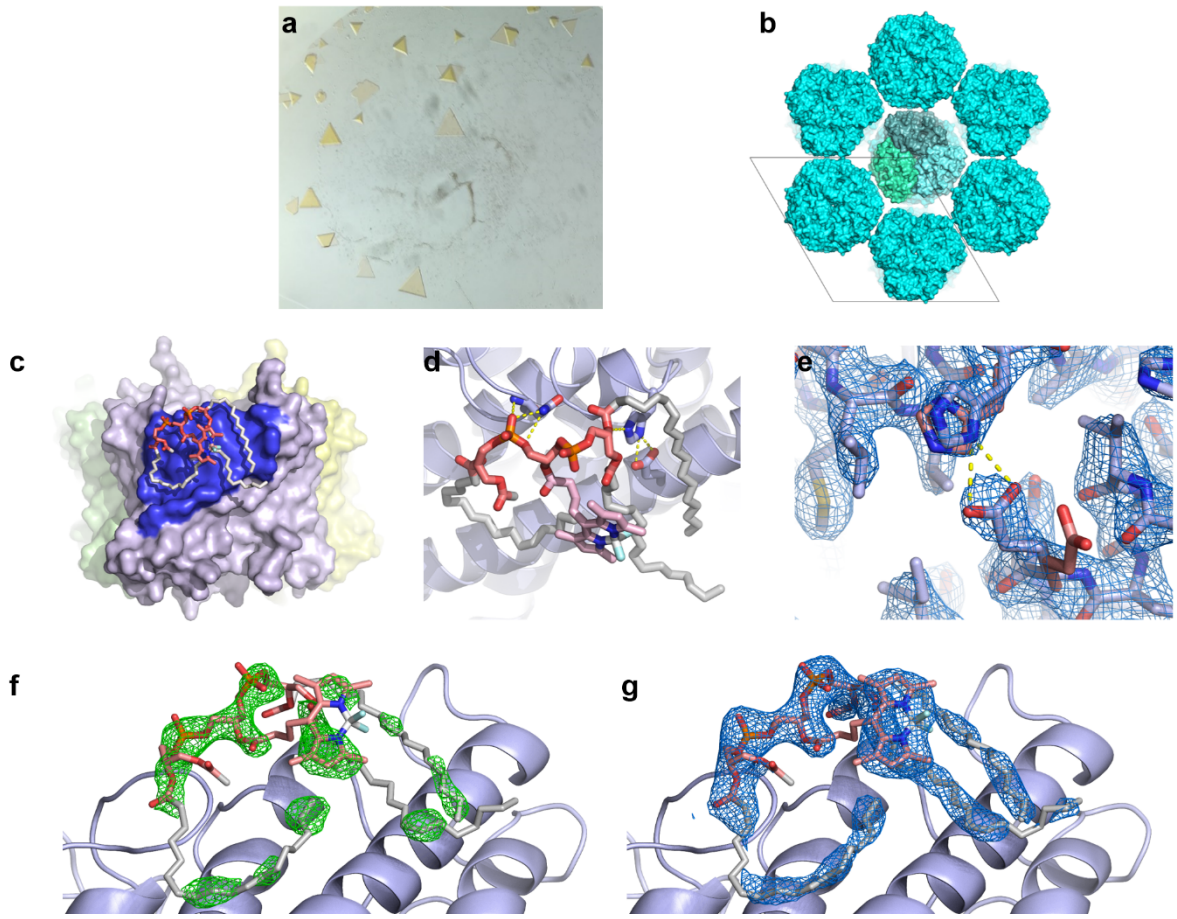

Figure S9 | Crystallographic analysis of AmtB bound to TFCDL. a, Photograph of AmtB crystals grown in the presence of TFCDL and POPE. **b,** Crystal packing symmetry viewing parallel to the c-axis. The unit cell is shown as a black line. Monomers within the trimeric complex are colored in one trimeric assembly for clarity. **c-d,** Same view as Fig. 3c and 3b but with the BODIPY headgroup of TFCDL intact. **e,** Electron density map ($2F_o$-F_c; σ = 1.7) of H156, E357 and surrounding residues of AmtB. The rearrangement of E357 to interact with H156 upon TFCDL binding is unique among the other AmtB structures, with a representative structure shown in light red (PDB: 1U7G). **f,** Simulated annealing omit map (F_o-F_c; σ = 3.7) with TFCDL omitted. **g,** Electron density map ($2F_o$-F_c; σ = 1.0) of TFCDL in the refined model.

Table S1 | Summary of X-ray data collection and refinement statistics.

	AmtB·TFCDL
Wavelength (Å)	0.979
Resolution Range (Å)	56.22 - 2.45 (2.54 - 2.45)
Space Group	H32
Unit Cell Parameters (Å;°)	$a = b = 138.8$, $c = 159.1$ $\alpha = \beta = 90$, $\gamma = 120$
Total Reflections	98128 (8983)
Unique Reflections	21583 (2125)
Multiplicity	4.5 (4.2)
Completeness (%)	98.8 (99.4)
***I/σ* (I)**	15.3 (2.8)
Wilson B-factor	48.9
R_{merge}[1]	0.066 (0.498)
R_{meas}[2]	0.073 (0.559)
$CC_{1/2}$	0.999 (0.871)
CC*[3]	1.0 (0.958)
Reflections used for R_{free}	1080 (107)
R_{cryst}[4]	0.1699 (0.2299)
R_{free}[5]	0.2125 (0.2780)
CC(work)	0.962 (0.904)
CC(free)	0.914 (0.877)
Number of non-hydrogen atoms	2832
macromolecules	2648
ligands	107
water	77
Protein residues	370
RMS(bonds; Å)	0.002
RMS(angles; °)	0.62
Ramachandran favoured (%)	97.0
Ramachandran allowed (%)	3.0
Ramachandran outliers (%)	0
Clashscore	1.29
Average B-factor (Å^2)	61.7
macromolecules	60.3
ligands	95.4
solvent	64.6

[1] $R_{merge} = \frac{\sum_{hkl}\sum_{i=1}^{n}|I_{i,hkl} - \bar{I}_{hkl}|}{\sum_{hkl}\sum_{i=1}^{n} I_{i,hkl}}$

[2] $R_{meas} = \frac{\sum_{hkl}\sqrt{\frac{n}{n-1}}\sum_{i=1}^{n}|I_{i,hkl} - \bar{I}_{hkl}|}{\sum_{hkl}\sum_{i} I_{i,hkl}}$

[3] $CC^* = \sqrt{\frac{2CC_{1/2}}{1+CC_{1/2}}}$

[4] $R_{crys} = \frac{\sum_{hkl}|F_{hkl}^{obs} - F_{hkl}^{calc}|}{\sum_{hkl} F_{hkl}^{obs}}$

[5] Same as R_{cryst} but with 5% of the reflections omitted.

Table S2 | Equilibrium binding constants and coupling factors for TFCDL with either POPC or POPE binding AmtB^{H156A}. Reported are the average and s.e.m. from repeated measurements (n = 3).

Lipid Species	k_D (μM)	R^2
KPOPC$_1$	8.5 ± 0.38	0.91
KPOPC$_2$	9.2 ± 0.29	
KPOPC$_3$	12.6 ± 5.47	
KPOPC$_4$	10.9 ± 0.64	
KPOPC$_5$	15.3 ± 2.03	
KTFCDL$_1$	20.5 ± 0.92	
KTFCDL$_2$	25.2 ± 1.89	
KTFCDL$_3$	14.8 ± 0.32	
KTFCDL$_4$	22.0 ± 5.68	
KTFCDL$_5$	18.4 ± 2.55	

Lipid Species	k_D (μM)	R^2
KPOPE$_1$	6.4 ± 0.27	0.98
KPOPE$_2$	9.5 ± 0.53	
KPOPE$_3$	9.9 ± 0.25	
KPOPE$_4$	18.9 ± 0.43	
KPOPE$_5$	14.8 ± 1.91	
KTFCDL$_1$	27.9 ± 0.13	
KTFCDL$_2$	41.1 ± 0.29	
KTFCDL$_3$	16.1 ± 1.25	
KTFCDL$_4$	78.9 ± 23.61	
KTFCDL$_5$	3.18 ± 1.38	

Supporting References

1. Cong X*, et al.* (2016) Determining Membrane Protein-Lipid Binding Thermodynamics Using Native Mass Spectrometry. *J Am Chem Soc* 138(13):4346-4349.
2. Laganowsky A*, et al.* (2014) Membrane proteins bind lipids selectively to modulate their structure and function. *Nature* 510(7503):172-175.
3. Subbarow CHFaY (1925) The colorimetric determination of phosphorus. *J. Biol. Chem.* 66:26.
4. P. S. Chen TYT, Huber Warner (1956) Microdetermination of Phosphorus. *Anal. Chem.* 28(11):3.
5. Laganowsky A, Reading E, Hopper JT, & Robinson CV (2013) Mass spectrometry of intact membrane protein complexes. *Nat Protoc* 8(4):639-651.
6. Allison TM*, et al.* (2015) Quantifying the stabilizing effects of protein-ligand interactions in the gas phase. *Nat Commun* 6:8551.